Available online at www.eccomasproceedia.org
Eccomas Proceedia COMPDYN (2019) 4079-4089

ECCOMAS
Proceedia

COMPDYN 2019
7th ECCOMAS Thematic Conference on
Computational Methods in Structural Dynamics and Earthquake Engineering
M. Papadrakakis, M. Fragiadakis (eds.)
Crete, Greece, 24–26 June 2019

SEISMIC RELIABILITY OF RC BUILDINGS MADE WITH EAF CONCRETES

Mariano Angelo Zanini[1], **Flora Faleschini**[1,2], **and Klajdi Toska**[1]

[1] Dept. of Civil, Environmental and Architectural Engineering, University of Padua.
Via Marzolo 9, 35131 Padua, Italy
e-mail: marianoangelo.zanini@dicea.unipd.it
e-mail: lorenzo.hofer@dicea.unipd.it

[2] Dept. of Industrial Engineering, University of Padua.
Via Gradenigo 6, 35131 Padua, Italy
e-mail: flora.faleschini@dicea.unipd.it

Abstract

The development of sustainable concretes is becoming an emerging issue in civil construction sector. The use of recycled aggregates is one way to fulfill sustainability goals in concrete industry, and among others, Electric Arc Furnace (EAF) slag aggregates has been proven to be promising. Past research demonstrated a significant increase of mechanical properties of EAF concretes when compared with ones made with natural aggregates (NA); however, at the same time, their use implies also an increase of self-weight loads. The present study aims therefore to investigate the seismic reliability of reinforced concrete frame buildings made with EAF, and compare it with the same structural configurations built with NA mixes, in order to show how the change in mechanical properties and self-weight can impact the seismic response of the analyzed case-studies.

Keywords: EAF slag, reinforced concrete moment frames, seismic fragility, seismic reliability.

ISSN:2623-3347
Peer-review under responsibility of the organizing committee of COMPDYN 2019.
doi: 10.7712/120119.7208.19855

1 INTRODUCTION

Construction waste reduction is one of the main goals construction industry has to face in the upcoming years [1]. Recycling and reuse are seen as the main policies for waste reduction disposal and a lot of studies and research has been done on achieving this objective. Recycled Aggregates (RAs) production is one of the main uses of Construction and Demolition Waste (C&DW) and their use is allowed in most countries around the world [3-5]. Among RAs from C&DW, recently, other kind of waste, mostly originating from industrial processes, have been object of research to evaluate their possible use to produce RAs or so-called industrial aggregates. Only in Europe, nearly 2.7 billion tonnes of natural aggregates are consumed each year [2]. Previous research has shown that among all industrial waste or by-products, those coming from steelmaking industry, particularly electric arc furnace (EAF) slag, offer the best performance when used in structural concrete. Particularly has been observed that EAF slag use enhances both mechanical strength [6-10] (i.e compressive strength, tensile strength and elastic properties) and durability [11-13] of concrete mixtures when compared to ordinary ones. Another difference worth highlighting is heavy-weight metals presence in the EAF slag composition which gives EAF concrete mixtures a higher specific weight with respect to NA mixtures. [14-15] have demonstrated that reinforced concrete (RC) elements with EAF slag aggregates manifest better flexural and shear capacity with respect to ordinary RC when tested to monotonic loading under four-point bending. Columns under uniaxial compression has shown a similar ductility to that of NA mixtures [17] while a higher shear strength of exterior beam-column joint is observed [18]. Experiments of EAF concrete joints under cyclic loading have shown a gain with respect to NA ones in terms of ductility, dissipated energy and reduced cracking patter. The same results were obtained even for a joint made with a minor cement amount [18]. Bond properties, between reinforcement and concrete, are also improved when using EAF slag aggregates [16]. Other beam-column joint conditions (i.e strong beam – weak column and strong column – weak beam situations) have been numerically investigated [19].

EAF concrete has found different applications, especially in gravity structures that require shielding from radiations where its high specific weight and high strength can be better exploited [20]. However, no studies have been made to investigate the efficacy of EAF slag concrete when applied in elevation RC structures, particularly, in seismic regions where an important change of the building mass can lead to a variation of the vibration modes and fundamental periods, impacting so the seismic loads acting in the structure elements.

Therefore, the present study aims to investigate this topic, analyzing the seismic response of code conforming RC frame buildings designed with ordinary NA concretes then replaced with three different EAF concrete classes characterized by different aggregates replacement ratios. For the mechanical properties' definition of EAF concrete mixtures a dataset of experimental tests based on two previous research works of some of the authors [21-22] is used. Mean mechanical properties, ratios of variation and self-weight were extracted via statistical processing for three EAF concrete classes (C1, C2, A) with respect to a benchmark mixture realized with NAs. For the purpose, three RC frame structures with three, six and nine stories were designed according to the current Italian Code for Constructions [5] for a medium-to-high seismic hazard site. From these an overall of 12 models resulting from the combinations of 3 structural configurations and 4 concrete mixes, were created. Fragility functions were then computed from the seismic responses of the analyzed configurations under a set of non-linear time history analysis (NLTHAs) and a seismic reliability assessment was carried out for all 12 combinations, investigating the variation of structural safety margins related to the use EAF concrete mixtures in replacement to a conventional NA concrete.

2 EAF SLAG AND ITS USE AS AGGREGATE IN STRUCTURAL CONCRETE

EAF slag properties depend on several factors, such as the type of steel to be produced, scrap composition, slag cooling method and speed, and further weathering process. Its composition includes mainly iron, calcium, silicon and aluminum oxides [23]. Usually, before the raw product is ready to be used as a recycled aggregate, it must pass through a weathering protocol [23] to reduce the volumetric instability of the matrix. The main properties of the slag for two size fractions compared, with a dolomitic aggregate, are reported in Table 1.

	Apparent density (kg/m3)	Water absorption (%)	Porosity (%)	shape
EAF slag 0-4 mm	3800	1.0 – 1.5	2.0	Crushed
EAF slag 4-16 mm	3950	<1.0	0.5 – 2-7	Crushed
NA 0-4 mm	2760	1.0 1.5	< 2.0	Roundish
NA 4-16 mm	2790	<0.5	0.9 – 1.8	Roundish

Table 1: Physical properties of EAF slag compared to dolomitic aggregate (NA).

The properties of the concrete matrix with EAF slag aggregates depends on type and amount of substitution. Generally coarse aggregates improve mechanical properties, while fine fraction affect is minor [12]. Workability of EAF concrete is highly reduced by high porosity and the crushed shape that characterizes the slag. Another important variation is observed on the specific weight of EAF concrete. Compared to a conventional NA concrete, the use of EAF slag can increase the specific weight of the matrix up to 15-20%. While gain in mechanical properties depends on slag type and fraction size, it seems that specific weight increase is almost constant and is not affected by these factors. Elastic modulus is also improved when using EAF slag. This is mainly because concrete elastic modulus depends mainly on the aggregates elastic modulus. The overall property improvements are also due to the interfacial transition zone between EAF aggregate and cementitious matrix. If a bad quality cementitious matrix or a high water/cement ratio is employed property enhancements are less important.

3 RC FRAME CODE-CONFORMING ANALYZED CASE STUDIES

To analyze the seismic response of different buildings built with EAF concrete three moment frame RC structures with 3-, 6-, and 9- stories were considered. The structures are characterized by a rectangular shape with five spans in the longitudinal direction and three in the transversal one. Span length is equal to 5 m in both directions.

The structures were designed in accordance with the Italian Building Code [5] considering a moderate-to-high seismic hazard site (Municipality of Pordenone, Northeast Italy) and a low ductility class (Class B). Seismic actions were computed from a dynamic linear analysis while beams and columns were designed accordingly using a C25/30 conventional concrete class.

4 THEORETICAL BACKGROUND ON SEISMIC RELIABILITY ANALYSIS

The occurrence of main shock events at a given site is assumed to be a Homogenous Poisson Process for the Performance-Based Earthquake Engineering (PBEE) framework [24]. So, the process of events causing structural failure is also a HPP and its unique parameter, failure rate λ_f, can be used for computing the failure probability at any time. The failure rate depends on the seismicity of the site (hazard curve λ_{im}) and on the structural behavior (fragility curve $P[f|im]$) [25-29]. λ_f is computed by applying the Total Probability Theorem as:

$$\lambda_f = \int_{im} P[f|im] \cdot |d\lambda_{im}| \quad (1)$$

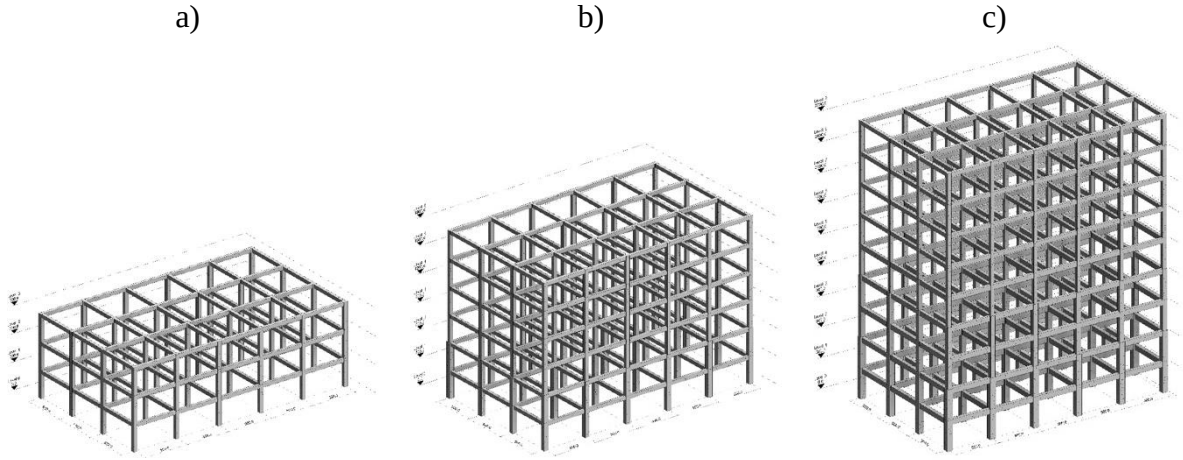

Figure 2: RC frame layouts analyzed: 3- (a), 6- (b) and 9-story (c) building archetypes.

4.1 Seismic hazard estimation

The so-called Probabilistic Seismic Hazard Analysis [30-31], for the computation of λ_{im} associates to each im value, the annual rate of events that exceed it at a given site. The seismicity of a given area di defined by three main components: the earthquake occurrence model, the spatial seismogenic model and the attenuation model. $|d\lambda_{\mathrm{im}}|$ represents the mean number of events per year with an intesity of exactly im and is obtained as:

$$|d\lambda_{\mathrm{im}}| = -\frac{d\lambda_{\mathrm{im}}}{d(im)} d(im) \quad (2)$$

On the other hand, $\lambda_{im}$is obtained via the following PSHA integral:

$$\lambda_{im} = \sum_{i=1}^{n_{SZ}} \nu_{m_{min,i}} \int_{m_{min,i}}^{m_{max,i}} \int_{r_{min,i}}^{r_{max,i}} P[IM > im|m,r] f_{M_i}(m) f_{R_i}(r)\, dm\, dr \quad (3)$$

where $\nu_{m_{min,i}}$ is the rate of occurrence of earthquakes greater than a suitable minimum magnitude $m_{min,i}$ of the i^{th} seismogenic zone *(SZ)*, $f_{M_i}(m)$ is the magnitude distribution for the i^{th} *SZ* and $f_{R_i}(r)$ is the distribution of the source i^{th}-to-site distance. Given a combination of magnitude m and distance r, $P[IM > im|m,r]$ is the probability to exceed im. The seismic hazard map for Italy is provided by the National Institute of Geology and Volcanology (INGV) [32]. To compute the failure rate a continuous hazard function is needed. Since INGV provides hazard data (values of the 16th, 50th and 84th percentile) only for nine return times, it is possible to fit the median values (i.e., the 50th percentile) with a quadratic function in the logarithmic space as:

$$\lambda(s) = k_0\, e^{(-k_1 \ln(s) - k_2 ln^2(s))} \quad (4)$$

In assessing seismic reliability, instead of the median hazard curve, it is more suitable to refer to the mean one which is possible to derive with the following equation:

$$\bar{\lambda}(s) = \lambda(s)\, e^{(\frac{1}{2}\beta_H^2)} \quad (5)$$

where β_H can be estimated as:

$$\beta_H = \frac{\ln(S_{84\%}) - \ln(S_{16\%})}{2} \quad (6)$$

4.2 Seismic fragility analysis

The fragility function ($P[f|im]$) represents the probability to reach and exceed a certain damage state given a specific intensity im. Several frameworks for fragility function estimation exits in literature, the most popular ones are the Incremental Dynamic analysis [33], the Cloud Analysis [34] and the Multi-Stripes Analysis [35].

In this work the Cloud Analysis method is adopted. The fragility parameters are estimated starting from a set of n natural ground motion records. The fragility function is computed as follows:

$$[f|im] = P\left[EDP > \overline{edp}|im\right] = 1 - P\left[EDP \leq \overline{edp}|im\right] = 1 - \Phi\left[\frac{ln(\overline{edp}) - ln(edp)}{\beta}\right] \quad (7)$$

$\overline{edp}$ is the median threshold value of the assumed structural limit state, and edp represents the median estimate of the demand that can be computed with a ln-linear regression model, as:

$$ln(edp) = a + b \cdot ln(im) \quad (8)$$

β is the standard deviation of the demand conditioned on im and can be estimated from the regression of the seismic demands as:

$$\beta_H = \frac{\ln(S_{84\%}) - \ln(S_{16\%})}{2} \quad (9)$$

5 SEISMIC RELIABILITY ASSESSENT OF THE ANALYZED EAF RC FRAME ARCHETYPES

NLTHAs were carried out with SeismoStruct software [36]. A diffused plasticity model, using a fiber section discretization, was adopted to consider material non-linearities. Unconfined and confined concrete was modeled via the Mander et al. [37] model whereas the Menegotto-Pinto [38] steel model was used for the non-linear behavior of rebars. EAF concrete characteristics are computed using the ratio coefficients in Table 2 and the reference concrete material (C25/30) characteristics.

	Class EAF-C1	Class EAF-C2	Class EAF-A
$\rho_{c,EAF} / \rho_{c,Ref}$	1.166	1.166	1.154
$f_{c,EAF} / f_{c,Ref}$	1.395	1.404	0.915
$f_{ct,EAF} / f_{ct,Ref}$	1.280	1.100	1.080
$E_{c,EAF} / E_{c,Ref}$	1.330	1.100	1.040

Table 2: Ratios between EAF and Reference concrete properties.

Fragility analysis is computed from a set of point data representing the Intensity Measure (IM) of a given seismic event and the corresponding non-linear response parameter (i.e Engineering Demand Parameter (EDP)). Since the Performance Based Earthquake Engineering was introduced, many researchers have tried to study IM and EDP parameters that best describe structure response under seismic excitation [39-41]. In the present paper, the chosen EDP parameter is the maximum interstory drift ratio (IDR) while the peak ground acceleration (PGA) is used as IM. In addition, four damage states: Slight, Moderate, Extensive and Complete, with corresponding EPD threshold of 0.4%, 0.8%, 1.5% and 3%, were defined.

Threshold values result similar to those proposed for ductile RC moment frame structures by [39] and were defined from non-linear static analysis. For the mid-rise and high-rise buildings, a reduction factor of respectively 2/3 and 1/2 as proposed by [42] was considered to account for higher mode effects and differences between average computed in a non-linear static analysis and maximum individual IDR from NLTHAs.

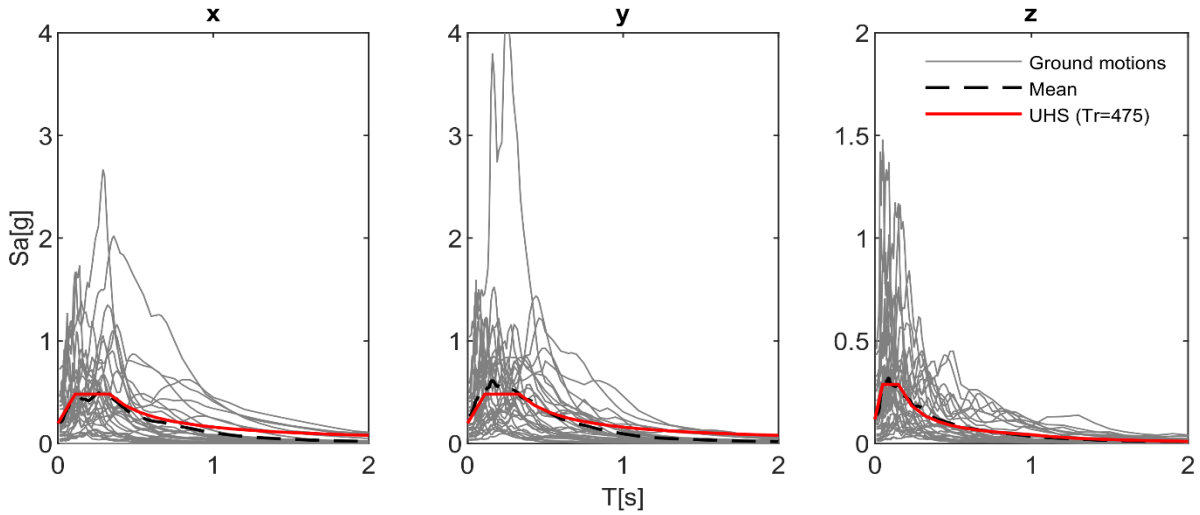

Figure 3: Selected seismic records: X- , Y- and Z- direction.

6 RESULTS AND DISCUSSION

For the NLTHAs a set of 30 natural unscaled ground motion records were adopted. In the seismic simulation all three components of the seismic wave, which spectral response is shown in figure 3, were considered. The structural response was then evaluated with respect to the four DSs previously defined, varying from Slight to Complete. Fragility functions were computed for each of the 12 cases, resulting from different geometrical and material combinations, using the Cloud Method described in Section 4.2.

Fragility curves for Slight, Moderate, Extensive and Complete damage are shown in Figure 4 in green, yellow, orange and red color respectively. Additionally, solid lines were used for frames realized with the reference concrete; instead, dotted, dashed and dash-dot lines were used for EAF-C1, EAF-C2 and EAF-A concretes, respectively.

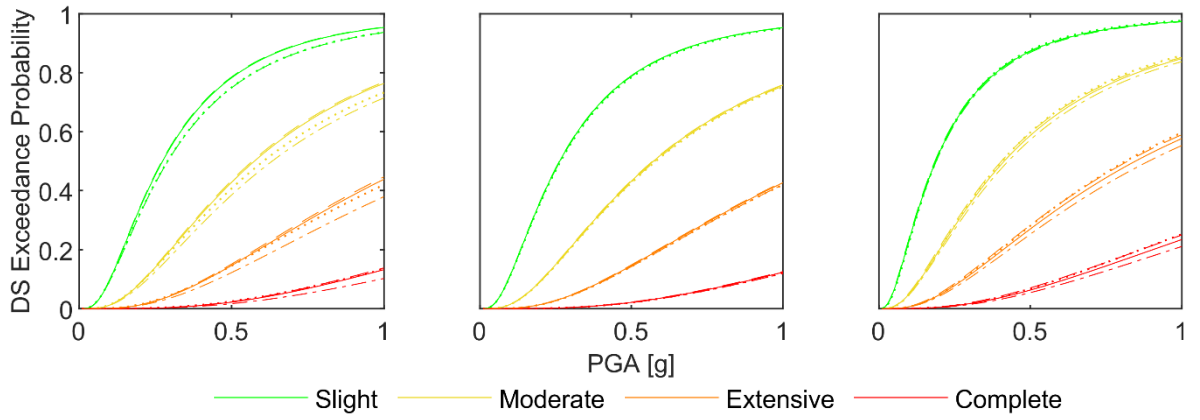

Figure 4: Slight, Moderate, Extensive and Complete DS fragility curves for 3- (a), 6- (b) and 9- (c) story RC frame archetypes (Solid - reference material (C25/30); Dotted - EAF-C1; Dashed - EAF-C2; Dash-dot – EAF-A).

A comparison of the seismic performance of structures built with the reference concrete and EAF concrete is given in Figure 4. It can be noted that the overall performance of EAF concrete structures is close to the performance of the reference material one. The 6- story model has shown almost the same response for all considered materials, proven by the overlapping fragility curves, while the 3- and 9- story curves tend to vary more when considering different materials. Comparing the fragility curves for the different geometrical configurations considered, is noted that 3- and 6- story buildings fragilities result similar for all DSs considered, while the 9 story building results more vulnerable under seismic solicitation with respect to the low- and mid-rise buildings.

Mean failure rates were also computed for all building frames (Table 3). When compared to the reference material the EAF concrete buildings report similar mean failure rate values. This confirms that in terms of safety margins with respect to seismic actions, buildings designed with ordinary concrete but built with EAF aggregates are exposed to almost the same risk as those realized with NAs ones. This highlights that NAs replacement with EAF aggregates, in the same structural system, has a small impact in terms of seismic reliability levels achieved. It is also observed that the mean failure rate for the 9-story building is almost twice the ones computed for the 3- and 6- story archetypes. This great difference may be affected by the reduced damage states EDP threshold adopted for the 9- story by considering it a high-rise building but it also points out that current code recommendations does not guarantee building design characterized by the same level of seismic reliability but often some differences can be observed, especially when comparing different rise buildings.

The construction of the three hypothesized models would require more than 2000 m^3 of concrete. In terms of environmental benefits, considering about 1700kg of NA/m^3 in a mix design for a reference concrete, nearly 3400 tons of NA could be saved if natural material would be fully replaced with EAF slag.

DS	Story	C25/30	C1-EAF	C2-EAF	A-EAF
Slight	3-	4.31E-03	4.28E-03	4.37E-03	4.22E-03
	6-	4.97E-03	4.91E-03	5.05E-03	4.94E-03
	9-	1.08E-02	1.02E-02	1.12E-02	1.08E-02
Moderate	3-	8.98E-04	9.23E-04	9.23E-04	8.27E-04
	6-	9.93E-04	9.77E-04	1.01E-03	9.76E-04
	9-	2.46E-03	2.39E-03	2.61E-03	2.34E-03
Extensive	3-	1.80E-04	1.93E-04	1.88E-04	1.55E-04
	6-	1.89E-04	1.85E-04	1.94E-04	1.83E-04
	9-	5.27E-04	5.30E-04	5.78E-04	4.80E-04
Complete	3-	2.43E-05	2.76E-05	2.58E-05	1.90E-05
	6-	2.36E-05	2.31E-05	2.45E-05	2.26E-05
	9-	7.71E-05	8.13E-05	8.80E-05	6.58E-05

Table 3: Comparison between mean failure rates derived for 3-, 6- and 9-story RC frame archetypes.

7 CONCLUSIONS

The main goal of this paper was to investigate the seismic performance of different code conforming RC-frame archetypes (3-, 6- and 9- stories) built with different substitution rates of NAs with EAF slag. The impact of EAG slag in weight and stiffness variation can change the

eigen values of the structure, therefore, seismic loads and global response of the building. A seismic reliability assessment was carried out and mean failure rates were computed for each combination of geometrical configuration and concrete type considered starting from the fragility functions derived with the cloud analysis for four DSs. Based on the results of the present study the following conclusions can be highlighted:

- Using materials that were proved to have higher mechanical strength than the reference one, might not improve the global seismic behavior of the structure.
- The seismic reliability analysis demonstrates that when replacing NAs of ordinary concrete with EAF ones the seismic safety levels achieved are comparable ti those of the same structural configuration built with ordinary concrete.
- For the low- and mid- rise buildings considered (3- and 6- stories) results showed a similar mean failure rate, while a significant variation was observed for the high-rise case (9- story). This marks out how current building codes may non ensure the same seismic reliability level for higher structures as for low- and mid- rise ones.

REFERENCES

[1] United Nations (2015) Resolution adopted by the General Assembly on 25 September 2015. 70/1. Transforming our world: the 2030 Agenda for Sustainable Development.

[2] European Aggregates Association (2017) Annual Review 2016-2017. (available online at: http://www.uepg.eu/uploads/Modules/Publications/uepg-ar2016-17_32pages_v10_18122017_pbp_ small.PDF).

[3] FHWA (1997) User Guidelines for Waste and Byproduct Materials in Pavement Construction. Federal Highway Administration Research and Technology Report no. FHWA-RD-97-148.

[4] EN 12620 (2008) Aggregates for concrete. Comité Européen de Normalisation, Brussels, Belgium.

[5] DM 17/01/2018 (2018) Aggiornamento delle Norme Tecniche per le Costruzioni, Roma, Italy. (in Italian).

[6] Pellegrino C., Gaddo V. (2009) Mechanical and durability characteristics of concrete containing EAF slag as aggregate. Cem Concr Compos 31(9): 663-671. doi: 10.1016/j.cemconcomp.2009.05.006.

[7] Arribas I., Santamaría A., Ruiz E., Ortega-López V., Manso J.M. (2015) Electric arc furnace slag and its use in hydraulic concrete. Constr Build Mater 90: 68-79. doi: 10.1016/j.conbuildmat.2015.05.003.

[8] Rondi L., Bregoli G., Sorlini S., Cominoli L., Collivignarelli C., Plizzari G. (2016) Concrete with EAF steel slag as aggregate: A comprehensive technical and environmental characterisation. Compos Part B 90: 195-202. doi: 10.1016/j.compositesb.2015.12.022.

[9] Liapis A., Anastasiou E.K., Papachristoforou M., Papayianni I. (2018) Feasibility Study and Criteria for EAF Slag Utilization in Concrete Products. J Sustain Metall 4(1): 68-76. doi: 10.1007/s40831-017-0152-2.

[10] Qasrawi H. (2014) The use of steel slag aggregate to enhance the mechanical properties of recycled aggregate concrete and retain the environment. Constr Build Mater 54: 298-304. doi: 10.1016/j.conbuildmat.2013.12.063.

[11] Faleschini F., Alejandro Fernández-Ruíz M., Zanini M.A., Brunelli K., Pellegrino C., Hernández-Montes E. (2015) High performance concrete with electric arc furnace slag as aggregate: mechanical and durability properties. Constr Build Mater 101, 113-121. doi: 10.1016/j.conbuildmat.2015.10.022

[12] Pellegrino C., Cavagnis P., Faleschini F., Brunelli K. (2012) Properties of concretes with black/oxidizing electric arc furnace slag aggregate. Cem Concr Compos 37: 232-240. doi: 10.1016/j.cemconcomp.2012.09.001.

[13] Ortega-López V., Fuente-Alonso J.A., Santamaría A., San-José J.T., Aragón Á. (2018) Durability studies on fiber-reinforced EAF slag concrete for pavements. Constr Build Mater 163: 471-481. doi: 10.1016/j.conbuildmat.2017.12.121.

[14] Pellegrino C., Faleschini F. (2013) Experimental behavior of reinforced concrete beams with electric arc furnace slag as recycled aggregate. ACI Mater. J. 110: 197-206.

[15] De Domenico D., Faleschini F., Pellegrino C., Ricciardi G. (2018) Structural behavior of RC beams containing EAF slag as recycled aggregate: Numerical versus experimental results. Constr Build Mater 171: 321-337. doi: 10.1016/j.conbuildmat.2018.03.128.

[16] Faleschini F., Santamaria A., Zanini M.A., San José J.-T., Pellegrino C. (2017) Bond between steel reinforcement bars and Electric Arc Furnace slag concrete. Mater Struct 50: 170. doi: 10.1617/s11527-017-1038-2.

[17] Lee J.-M., Lee Y.-J., Jung Y.-J., Park J.-H., Lee B.-S., Kim K.-H. (2018) Ductile capacity of reinforced concrete columns with electric arc furnace oxidizing slag aggregate. Constr Build Mater 162: 781-793. doi: 10.1016/j.conbuildmat.2017.12.045.

[18] Faleschini F., Hofer L., Zanini M.A., Dalla Benetta M., Pellegrino C. (2017) Experimental behavior of beam-column joints made with EAF concrete under cyclic loading. Eng Struct 139: 81-95. doi: 10.1016/j.engstruct.2017.02.038.

[19] Faleschini F., Bragolusi P., Zanini M.A., Zampieri P., Pellegrino C. (2017) Experimental and numerical investigation on the cyclic behavior of RC beam column joints with EAF slag concrete. Eng Struct 152: 335-347. doi: 10.1016/j.engstruct.2017.09.022.

[20] Pomaro B., Gramegna F., Cherubini R., De Nadal V., Salomoni V., Faleschini F. (2019) Gamma-ray shielding properties of heavyweight concrete with Electric Arc Furnace slag as aggregate: An experimental and numerical study. Constr Build Mater 200: 188-197.

[21] Pellegrino C., Faleschini F. (2016) Experimental Database of EAF Slag Use in Concrete. in: Sustainability Improvements in the Concrete Industry. Springer, Switzerland. doi: 10.1007/978-3-319-28540-5.

[22] Zanini M.A. (2019) Structural reliability of bridges realized with reinforced concretes with electric arc furnace slag aggregates. Eng Struct xx: yy-zz (accepted).

[23] Santamaria A., Faleschini F., Giacomello G., Brunelli K., San José J.T., Pellegrino C., Pasetto M. (2018) Dimensional stability of electric arc furnace slag in civil engineering applications. J Clean Prod 205: 599-609. doi: 10.1016/j.jclepro.2018.09.122.

[24] Cornell C.A., Krawinkler H. (2000) Progress and challenges in seismic performance assessment. PEER Centre News, 3(2): 1-3.

[25] Castaldo, P., Palazzo, B., Alfano, G., Palumbo, M.F. (2018) Seismic reliability-based ductility demand for hardening and softening structures isolated by friction pendulum bearings, Structural Control and Health Monitoring 25(11),e2256.

[26] Castaldo, P., De Iuliis, M. (2014) Effects of deep excavation on seismic vulnerability of existing reinforced concrete framed structures, Soil Dynamics and Earthquake Engineering 64, 102-112.

[27] Castaldo, P., Mancini, G., Palazzo, B. (2018) Seismic reliability-based robustness assessment of three-dimensional reinforced concrete systems equipped with single-concave sliding devices, Engineering Structures 163, 373-387.

[28] Castaldo, P., Ripani, M., Priore, R.L. (2018) Influence of soil conditions on the optimal sliding friction coefficient for isolated bridges, Soil Dynamics and Earthquake Engineering 111, 131-148.

[29] Castaldo, P., Palazzo, B., Perri, F. (2016) Fem simulations of a new hysteretic damper: The dissipative column, Ingegneria Sismica, 33(1), 34-45.

[30] Cornell C. (1968) Engineering seismic risk analysis. Bull Seismol Soc Am 58(5): 1583-1606.

[31] McGuire R.K. (1995) Probabilistic seismic hazard analysis and design earthquakes: closing the loop. Bull Seismol Soc Am 85(5): 1275-1284.

[32] INGV. Interactive Seismic Hazard Maps. Available at: http://esse1-gis.mi.ingv.it/s1_en.php (last access 04/03/2019).

[33] Vamvatsikos D., Cornell C.A. (2004) Applied incremental dynamic analysis. Earthquake Spectra, 20(2):523–553. doi: 10.1193/1.1737737.

[34] Jalayer F., Cornell C.A. Direct probabilistic seismic analysis: implementing non-linear dynamic assessments. Stanford University, 2003.

[35] Baker J.W. (2015) Efficient analytical fragility function fitting using dynamic structural analysis. Earthquake Spectra, 31(1): 579–599. doi: 10.1193/021113EQS025M.

[36] SeismoSoft (2013) SeismoStruct – a computer program for static and dynamic nonlinear analysis of frames structures. Available at: http://www.seismosoft.com.

[37] Mander J.B., Priestley M.J.N., Park R. (1988) Theoretical stress-strain model for confined concrete. Journal of Structural Engineering, 114(8): 1804-1826.

[38] Menegotto M., Pinto P.E. (1973) Method of analysis for cyclically loaded reinforced concrete plane frames including changes in geometry and non-elastic behavior of elements under combined normal force and bending. Proceedings IABSE Symposium of Resistance and Ultimate Deformability of Structures Acted on by Well Defined Repeated Loads, International Association of Bridge and Structural Engineering, Lisbon, Portugal, Vol. 13: 15-22.

[39] Whittaker A., Deierlein G. G., Hooper J., Merovich A. (2004) Engineering demand parameters for structural framing systems. Task 2.2 report for the ATC-58 project, Applied Technology Council (available from www.ATCouncil.org), Redwood City, California.

[40] Ghobarah, A. (2004) On drift limits associated with different damage levels. International workshop on Performance based design: concepts and implementations, 28 June- 1 July 2004.

[41] Stocchi A., Richard B. (2019) Sensitivity of engineering demand parameters as a function of structural typology and assessment method. Nuclear Eng Des 343: 151-165. doi: 10.1016/j.nucengdes.2019.01.006.

[42] FEMA (2012) Earthquake Model, Hazus-MH 2.1 Technical Manual. Federal Emergency Management Agency, Washington DC, US (available at: www.fema.gov/plan/prevent/hazus).